Cardiovasc Intervent Radiol (2017) 40:822–830
DOI 10.1007/s00270-017-1568-6

Extrahepatic Arteries Originating from Hepatic Arteries: Analysis Using CT During Hepatic Arteriography and Visualization on Digital Subtraction Angiography

Kumi Ozaki[1] · Satoshi Kobayashi[2] · Osamu Matsui[1] · Tetsuya Minami[1] · Wataru Koda[1] · Toshifumi Gabata[1]

Received: 9 October 2016 / Accepted: 2 January 2017 / Published online: 12 January 2017

Abstract
Purpose To investigate the prevalence and site of origin of extrahepatic arteries originating from hepatic arteries on early phase CT during hepatic arteriography (CTHA) was accessed. Visualization of these elements on digital subtraction hepatic angiography (DSHA) was assessed using CTHA images as a gold standard.
Materials and Methods A total of 943 patients (mean age 66.9 ± 10.3 years; male/female, 619/324) underwent CTHA and DSHA. The prevalence and site of origin of extrahepatic arteries were accessed using CTHA and visualized using DSHA.
Results In 924 (98.0%) patients, a total of 1555 extrahepatic branches, representing eight types, were found to originate from hepatic arteries on CTHA. CTHA indicated the following extrahepatic branch prevalence rates: right gastric artery, 890 (94.4%); falciform artery, 386 (40.9%); accessory left gastric artery, 161 (17.1%); left inferior phrenic artery (IPA), 43 (4.6%); posterior superior pancreaticoduodenal artery, 33 (3.5%); dorsal pancreatic artery, 26 (2.8%); duodenal artery, 12 (1.3%); and right IPA, 4 (0.4%). In addition, 383 patients (40.6%) had at least one undetectable branch on DSHA. The sensitivity, specificity, and accuracy of visualization on DSHA were as follows: RGA, 80.0, 86.8, and 80.4%; falciform artery, 53.9, 97.7, and 80.0%; accessory LGA, 64.6, 98.6, and 92.3%; left IPA, 76.7, 99.8, and 98.7%; PSPDA, 100, 99.7, and 99.9%; dorsal pancreatic artery, 57.7, 100, and 98.8%; duodenal artery, 8.3, 99.9, and 98.7%; and right IPA, 0, 100, and 99.6%, respectively.
Conclusion Extrahepatic arteries originating from hepatic arteries were frequently identified on CTHA images. These arteries were frequently overlooked on DSHA.

Keywords Extrahepatic arteries originating from hepatic arteries · CT during hepatic arteriography · Digital subtraction hepatic angiography · Transcatheter arterial chemoembolization

Introduction

Transcatheter arterial chemoembolization, hepatic arterial infusion chemotherapy, and radioembolization are valuable therapeutic options for unresectable hepatic tumors, particularly hepatocellular carcinoma (HCC) [1–3]. Chemotherapeutic drugs or particles used in these therapies can effectively induce tumor necrosis, but may also cause unwanted complications in nontarget organs [4] such as gastroduodenal ulceration or erosion associated with the gastric or duodenal artery [5]; abdominal wall injury, pain, or skin rash associated with the falciform artery [6]; pancreatitis associated with the pancreatic artery [7]; and shoulder pain, pleural effusion, or basal atelectasis associated with the inferior phrenic artery (IPA) [8]. These complications may be induced by inflow into unexpected or extrahepatic branches that arise from the intrahepatic arterial circulation. Therefore, identification of extrahepatic branches is important for the optimization of selective transarterial therapies.

✉ Kumi Ozaki
ozakik-rad@umin.org

[1] Department of Radiology, Kanazawa University Graduate School of Medical Science, 13-1 Takara-machi, Kanazawa 920-8640, Japan

[2] Department of Quantum Medicine Technology, Kanazawa University Graduate School of Medical Science, Kanazawa, Japan

However, digital subtraction hepatic angiography (DSHA) has insufficient spatial resolution and therefore may fail to detect the occasionally fine extrahepatic branches [9–11]. In addition, hepatic arterial flow increases as cirrhosis and portal hypertension progress, resulting in poorer visualization of small branches of the hepatic artery on DSHA.

Angiography-assisted CT, including CT during arterial portography (CTAP) and CT during hepatic arteriography (CTHA), is used in addition to angiography when performing transarterial liver therapies. These modalities have been adopted as the most sensitive HCC detection modalities [12–14]. In addition, although DSA depicts only arterial system, CT depicts both arterial system and surrounding organs; therefore, CTHA is expected to extensively detect the intrahepatic vasculature regardless of cirrhotic progression and could be adopted as a standard of reference because of its ability to indicate the accurate site of origin, enhancing vessels, and vascular territories or target organs. Therefore, we have adapted early-phase CTHA images not only to detect small nodules, but also to depict thin arteries.

The purpose of this study was to investigate the prevalence and site of origin of extrahepatic arteries on early-phase CTHA and to assess the visualization of these elements on DSHA using the data of early-phase CTHA as a gold standard, at different cirrhotic stages.

Materials and Methods

Patients

This retrospective study was approved by our institutional ethics committee, and all patients provided informed consent for the use of their CT images and clinical data for scientific research purposes.

From April 2007 to January 2010, 1204 consecutive patients underwent angiographic examinations, including DSHA and CTHA, for the further evaluation and/or treatment of hepatic tumors. Patients were excluded if they had a history of surgical or endovascular procedures ($n = 232$), severe celiac axis stenosis ($n = 14$), severe deformity due to an advanced tumor or inflammation ($n = 12$), or a requirement for carbon dioxide-based angiography because of iodine allergy ($n = 3$). Other exclusion criteria included difficulty in evaluating small extrahepatic arteries behind prominent tumor vascularity and staining, possible abnormal anastomosis or occlusion as a result of arterial obstruction after embolization, and possible non-visualization of extrahepatic arteries on angiography as a result of reversed flow in the presence of collateral circulation.

Nine hundred and forty-three patients (619 men and 324 women) met the inclusion criteria. The average age was 66.9 ± 10.3 years (range 19–89 years), with average ages of 65.8 ± 10.4 years (range 19–83 years) and 68.9 ± 9.7 years (37–89 years) for men and women, respectively. The indication for angiography and CTHA was a need for preoperative hepatic tumor evaluation. Preoperative or tentative diagnoses included hepatocellular carcinoma ($n = 786$), hepatic metastasis ($n = 122$), cholangiocellular carcinoma ($n = 13$), and other ($n = 22$). The background liver was normal in 157 patients (16.6%), whereas 187 patients had chronic hepatitis (19.8%) and 599 had cirrhosis (65.3%).

Angiographic and CTHA Examinations

All examinations were performed using standard angiographic equipment (IVR-CT/Angio System, InfinixCelevei; Toshiba Medical Systems, Tokyo, Japan). Celiac and superior mesenteric arteriography was performed via selective catheterization using a 4-F shepherd hook catheter (Terumo, Tokyo, Japan). Selective common hepatic arteriography (CHA) was performed using a 4-F or 3-F straight catheter or 2.0- to 2.7-F microcatheter. In cases with celiac axis or hepatic artery variations, selective replacement or accessory left hepatic or right hepatic arteriography was performed with a microcatheter. The total contrast medium volume and injection rate (iohexol, Omnipaque 350, Daiichi-Sankyo Pharmaceutical, Tokyo, Japan) were 20 mL and 4 mL/s, respectively, for celiac and superior mesenteric arteriography and 10–12 mL and 1.5–2.0 mL/s, respectively, for selective CHA ($n = 717$) or left hepatic and/or right hepatic arteriography ($n = 226$).

CTAP and CTHA were performed after arteriography, using the following scanning parameters: number of detector rows, 64; section thickness, 0.5 mm; pitch factor, 0.641; reconstruction intervals, 0.5 mm; gantry rotation time, 0.75 s; tube voltage, 120 kVp; and the tube mA determined automatically. For CTAP, CT scanning began 24 s after an infusion of 50 mL of iohexol at 1.8 mL/s was begun. Immediately before the injection of contrast medium, 5 μg of prostaglandin E1 (Palux, Taisyo, Tokyo, Japan) was injected into the superior mesenteric artery. CTHA began 7 s after initiating iohexol injection (1.5–2 mL/s); infusion continued until 5 s after early-phase CTHA scanning was completed. Thirty seconds after contrast material infusion finished (about 62–67 s after the infusion began), late-phase scanning commenced. The scanning time (approximately 20–25 s) varied according to the individual liver size. The total amount of non-diluted contrast medium varied according to the following equation: (early-phase scanning time + 12 s) × injection rate. Angiographic procedures were performed by radiologists who had >10 years of experience performing abdominal angiography.

Definition of Extrahepatic Arteries Originating from Hepatic Arteries

An extrahepatic artery was defined as an artery arising from the proper hepatic artery (PHA) or its distal branches or from CHA within 2 cm of the PHA bifurcation, which supplies organs and areas other than the hepatic parenchyma. These branches require attention to ensure the optimization of selective transarterial catheterization and block the passage of chemotherapeutic drugs or obstructing particles. In this study, we did not include the cystic artery as an extrahepatic artery. This artery almost always exists and can supply the hepatic parenchyma adjacent to the gallbladder bed, and the assessment of the prevalence was unnecessary. Furthermore, we should access the number of cystic arteries because it is not necessarily only one. Considering the purpose of this study, the cystic artery is a little different from other extrahepatic arteries. We adopted the term "middle hepatic artery (MHA)" to indicate an artery that originated beside the left hepatic artery (LHA) and supplied the medial liver segment. A4 was used to designate the artery arising from LHA to supply the medial segment.

Image Evaluation

DSHA and early-phase CTHA images were reviewed by a radiologist with >12 years of experience in abdominal imaging to determine the presence and site of origin of extrahepatic branches arising from the intrahepatic arterial circulation. For cases in which it was difficult to identify each artery, decisions were made in consensus with a senior radiologist with >20 years of experience in abdominal radiology. All images were reviewed using digital image analysis software (EV Insite version 2.10.7.91; PSP Corporation, Tokyo, Japan), which allowed optional cross-sectional maximal intensity projection. Basically, we adapted the slab thickness of 20 mm and reconstruction interval of 2 mm. When necessary, thinner slice and shorter interval were applied for image analysis of interested region.

On CTHA images, extrahepatic arteries were identified based on contrast enhancement of the corresponding vascular territories and their characteristic anatomical courses. On DSHA images, the presence or absence of extrahepatic arteries was assessed based on the arteries' characteristic courses and contrast enhancement of the corresponding vascular territories, with reference to several previous studies [4–11, 15–25]. The prevalence and site of origin of the extrahepatic branches were accessed on both CTHA and DSHA images. We evaluated visualization on DSHA using CTHA as the standard of reference, and accurate angiographic detection was defined as the detection of both the vessels and their sites of origin. The sensitivity, specificity, and accuracy of extrahepatic artery visualization on DSHA were calculated using CTHA findings as the standard of reference.

Results

In 924 (98.0%) of the 943 study patients, 1555 extrahepatic branches, representing eight types, were found to originate from the hepatic arteries. Four hundred and ten patients (43.5%) had one extrahepatic branch, 406 (43.1%) had two branches, and 108 (11.5%) had three or more branches. The following artery prevalence rates were determined on CTHA images: right gastric artery (RGA), 890 (94.4%); falciform artery, 386 (40.9%); accessory left gastric artery (LGA), 161 (17.1%); left IPA, 43 (4.6%); posterior superior pancreaticoduodenal artery (PSPDA), 33 (3.5%); dorsal pancreatic artery, 26 (2.8%); duodenal artery, 12 (1.3%); and right IPA, 4 (0.4%) (Table 1; Figs. 1, 2, 3, 4, 5, 6).

On DSHA images, 383 patients (40.6%) had at least one undetectable branch; of these, 303 (32.1% of the total), 66 (7.0%), nine (1.0%), and five (0.5%) had one, two, three, and four undetectable branches, respectively. Using these data, sensitivity, specificity, and accuracy were calculated for each artery on DSHA. The values were 80.0% (712/890), 86.8% (46/53), and 80.4% (758/943), respectively, for RGA (Fig. 1); 53.9% (206/382), 97.7% (548/561), and 80.0% (754/943), respectively, for the falciform artery (Fig. 1); 64.6% (104/161), 98.6% (771/782), and 92.3% (875/943), respectively, for accessory LGA (Fig. 2); and 76.7% (33/43), 99.8% (898/900), and 98.7% (931/943), respectively, for the left IPA (Fig. 3). Additional corresponding values were 100% (33/33), 99.7% (908/911), and 99.9% (941/943), respectively, for PSPDA; 57.7% (15/26), 100% (917/917), and 98.8% (932/943), respectively, for the dorsal pancreatic artery (Fig. 4); 8.3% (1/12), 99.9% (930/931), and 98.7% (931/943), respectively, for the duodenal artery (Fig. 5); and 0% (0/4), 100% (939/939), and 99.6% (939/943), respectively, for the right IPA (Fig. 6) (Table 2).

Discussion

In our study, 924 (98.0%) patients presented with at least one extrahepatic branch that had originated from an intrahepatic artery; eight types of extrahepatic branches were observed, and their frequencies were determined using CTHA images. In contrast, 383 (40.6%) patients had at least one undetectable branch on DSHA images. Our results revealed obviously poorer visualization of extrahepatic arteries on DSHA images when CTHA was used as the

Table 1 Prevalence and site of origin of the extrahepatic arteries originating from hepatic arteries determined using CT during hepatic arteriography

	RGA	Falciform artery	Accessory LGA	Left IPA	PSPDA	Dorsal pancreatic artery	Duodenal artery	Right IPA
Number of arteries	890 (94.4%)	386 (40.9%)	161 (17.1%)	43 (4.6%)	33 (3.5%)	26 (2.8%)	12 (1.3%)	4 (0.4%)
Prevalence of site of origin	PHA ($n = 582$)	A4 ($n = 189$)	LHA[b] ($n = 140$)	LHA[b] ($n = 41$)	PHA ($n = 26$)	CHA ($n = 15$)	PHA ($n = 9$)	A1 ($n = 2$)
	LHA ($n = 200$)	A3 ($n = 114$)	PHA ($n = 6$)	A3 ($n = 1$)	RHA ($n = 6$)	PHA ($n = 6$)	MHA ($n = 2$)	Posterior branch ($n = 1$)
	MHA ($n = 30$)	MHA ($n = 53$)	A2 separately originated from CHA ($n = 5$)	A2 separately originated from LGA ($n = 1$)	MHA ($n = 1$)	Replaced RHA originated from SMA ($n = 3$)	CHA/PHA ($n = 1$)	LHA ($n = 1$)
	RHA ($n = 16$)	LHA ($n = 19$)	RHA ($n = 2$)			LHA ($n = 1$)		
	PHA/GDA ($n = 34$)	A3 + A4 ($n = 4$)	A2 ($n = 2$)			RHA ($n = 1$)		
	CHA ($n = 13$)	RHA[a] ($n = 3$)	A3 + A4 ($n = 1$)					
	A4 ($n = 5$)	A2 ($n = 2$)	CHA ($n = 1$)					
	A2 separately originated from CHA ($n = 3$)	PHA ($n = 1$)	RHA originated from CHA ($n = 1$)					
	A4 separately originated from CHA ($n = 2$)	A3 separately originated from replaced LHA arising from LGA ($n = 1$)	A4 separately originated from CHA ($n = 1$)					
	A3 + A4 ($n = 2$)							
	A2 + A3 ($n = 1$)							
	A3 ($n = 1$)							
	A3 separately originated from CHA ($n = 1$)							

[a] In two patients, the falciform artery originated from RHA as a common trunk with the cystic artery

[b] In nine patients, the left IPA originated from LHA as a common trunk with the accessory LGA

RGA right gastric artery, *LGA* left gastric artery, *IPA* inferior phrenic artery, *PSPDA* posterior superior pancreaticoduodenal artery, *CHA* common hepatic artery, *GDA* gastroduodenal artery, *MHA* middle hepatic artery, *RHA* right hepatic artery

standard of reference, although there was a slight difference in the degree of visualization between each branch.

The prevalence rates of falciform artery (40.9%) and accessory LGA (17.1%) were similar to those reported in previous CTHA-based studies of Asian populations [9, 10], and the visualization of accessory LGA on DSHA was also similar to that reported in previous studies when CTHA was used as the standard of reference [9]. No other previous reports have described the prevalence of extrahepatic arteries using CHTA. Notably, the prevalence rates of RGA (94.4%) and falciform artery (40.9%) on CTHA images in the present study were higher than those reported in a previous angiographic study (78.4 and 2–25%, respectively) [10, 16]. Considering the sensitivity of these two arteries, our higher prevalence indicated that we overlooked these arteries on DSHA.

The prevalence rates of left IPA (4.6%) and PSPDA (3.5%) on CTHA images were slightly lower than those

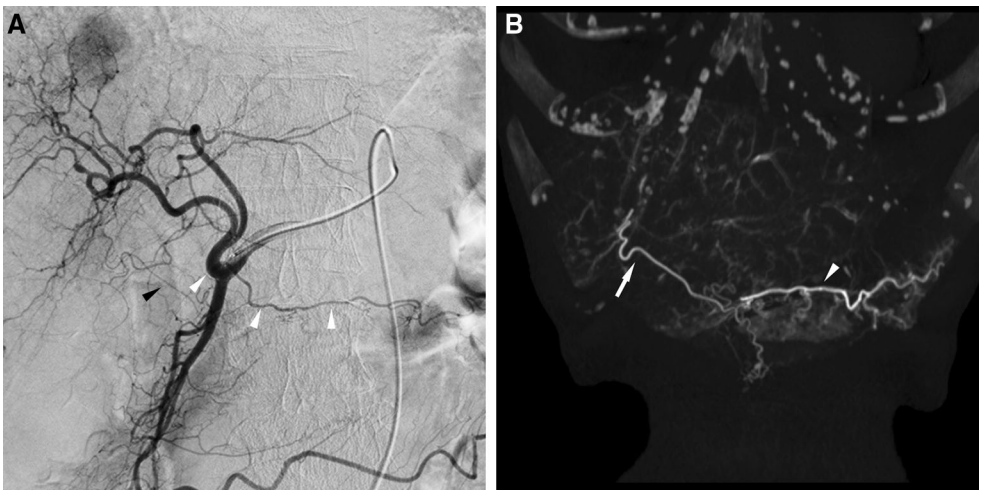

Fig. 1 Images of the right gastric artery and falciform artery in an 80-year-old woman with hepatitis C virus-related cirrhosis. **A** The right gastric artery originated from the proper hepatic artery (*white arrowheads*) and is clearly detectable on a common hepatic arteriogram. Another extrahepatic branch was missed during the first blind interpretation. The falciform artery (*black arrowhead*) has been retrospectively identified, although the site of origin is unclear. **B** Coronal CT hepatic angiography image (maximum intensity projection) clearly shows both the falciform artery (*arrows*) originating from A3 and the right gastric artery (*arrowhead*)

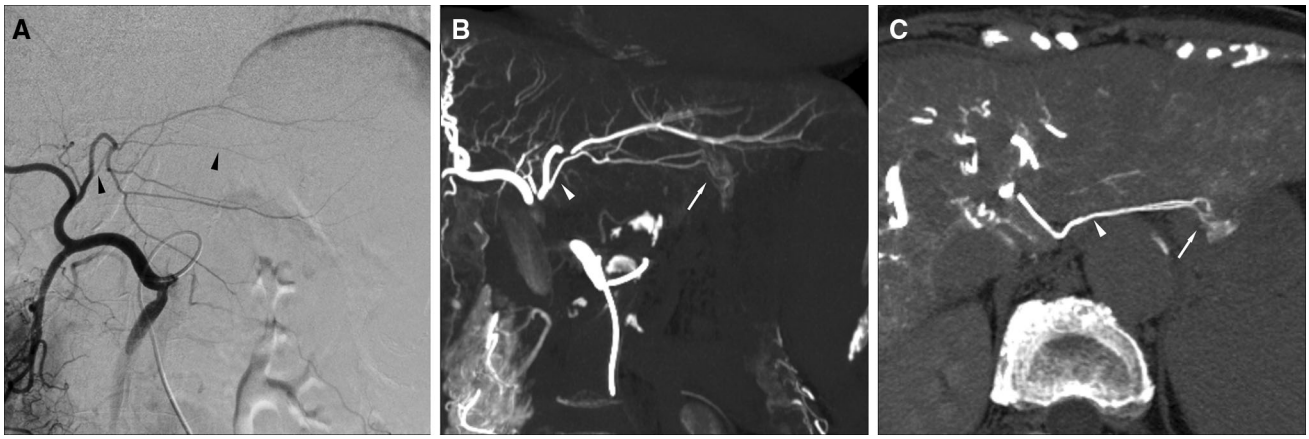

Fig. 2 Images of the accessory left gastric artery in a 77-year-old woman with hepatitis C virus-related cirrhosis. **A** The common hepatic artery arises from the superior mesenteric artery. The extrahepatic branch was missed during the first blind interpretation. The accessory left gastric artery (*black arrowheads*) was retrospectively identified, and gastric wall staining is unclear. **B** Coronal CT hepatic angiography (CTHA) image (maximum intensity projection) clearly shows the accessory left gastric artery with its origin from the left hepatic artery (*arrowhead*) and gastric wall staining (*arrow*). **C** Axial CTHA image (maximum intensity projection) clearly shows that the accessory left gastric artery runs through a fissure of the ligamentum venosum (*arrowhead*) and gastric wall staining (*arrow*)

reported in a previous angiographic study of an Asian population (5 and 7.2%, respectively) [16]. Because detection based on CHTA images was assumed to be accurate, the specificity of our results indicated that we had mistakenly identified different branches.

No previous reports have described the prevalence rates of the dorsal pancreatic artery, duodenal artery, and right IPA using DSHA or CTHA. This lack of reporting may be attributable to a previous failure to recognize these arteries, which exhibit low sensitivity on DSHA, as extrahepatic arteries. Typically, the dorsal pancreatic artery arises from CHA near the celiac axis [24] and does not require attention because it is sufficiently proximal to avoid collateral damage. In rare cases, the dorsal pancreatic artery originates from a distal site of PHA or CHA, as shown in our study. The duodenal arteries most commonly originate from PSPDA or GDA and are rarely identified separately. These variations are difficult to detect on DSHA, as shown in our study and a previous systematic angiographic study [16]. The right IPA most commonly originates from the aorta or celiac axis independently or as a common trunk with the left IPA. Various other sites of origin, including the renal, left gastric, hepatic, and superior mesenteric arteries, are less frequently observed [19]. The right IPA,

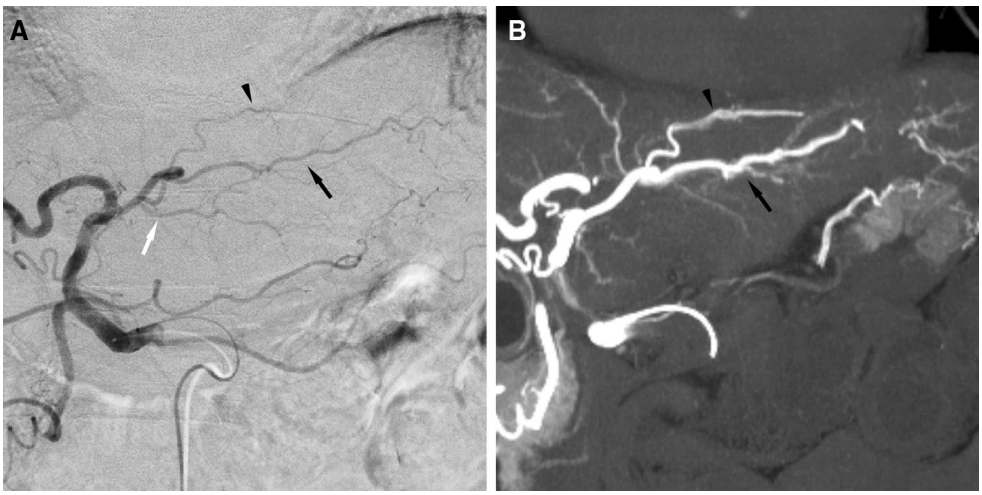

Fig. 3 Images of the left inferior phrenic artery in a 73-year-old man with alcoholic cirrhosis. **A** The extrahepatic branch was missed on the common hepatic arteriogram during the first blind interpretation. The left inferior phrenic artery (*black arrowhead*) was retrospectively identified (A2; *black arrow*, A3; *white arrow*). **B** Coronal CT hepatic angiography (CTHA) image (maximum intensity projection) clearly shows the left inferior phrenic artery (*arrowhead*) arising from the distal sight of the left hepatic artery and hepatic artery (A2) (*arrow*)

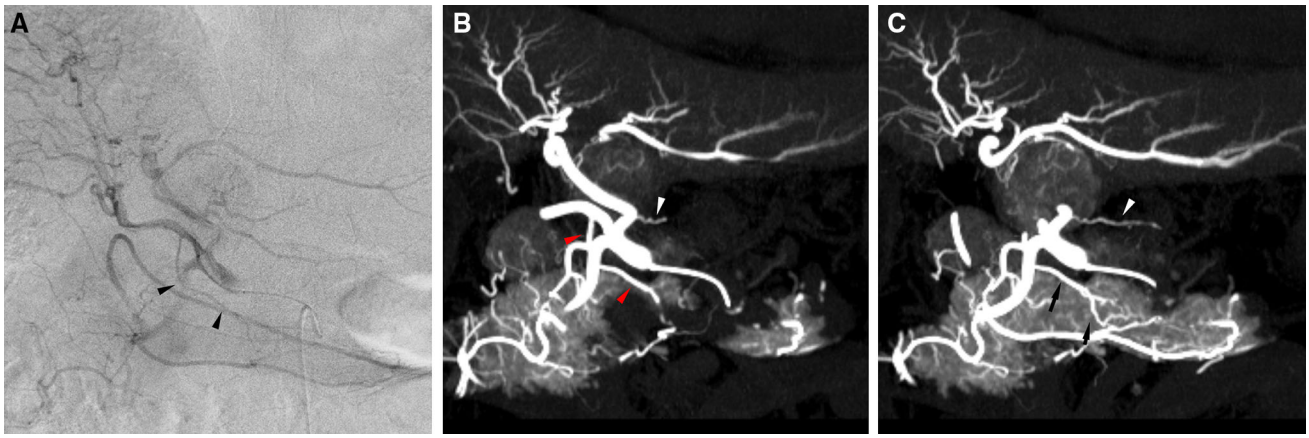

Fig. 4 Images of the dorsal pancreatic artery in a 72-year-old man with a normal liver. **A** A branch arising from the right hepatic artery (*black arrowheads*) was identified on the common hepatic arteriogram, although the vascular territory was uncertain. Another extrahepatic branch was missed during the first blind interpretation. **B**, **C** Coronal CT hepatic angiography (CTHA) images (maximum intensity projection) clearly show the branch arising from the right hepatic artery supplies the pancreatic body (*red arrowheads* and *black arrows*) and was found to be the dorsal pancreatic artery. The right gastric artery arising from the left hepatic artery is also clearly depicted (*white arrowheads*)

which originates from the hepatic artery, was also difficult to detect on DSHA in both our study and a previous systematic angiographic study.

Several factors were speculated to cause poorer visualization on DSHA images. The angiographic quality itself, which was influenced by several factors such as the physical frame, contrast material volume and injection, and radiation dose, is expected to strongly affect visualization. Similarly, the artery diameter would also be implicated as visualization of thinner arteries on DSHA was easily disturbed. In addition, conventional two-dimensional arteriography, which commonly uses coronal images, may fail to discriminate overlapping ventrodorsal branches. Furthermore, two-thirds of our study population presented with cirrhosis. As cirrhotic changes progressed in these patients, hepatic arteriograms revealed tortuous and dilated peripheral hepatic branches together with morphometric and atrophic parenchymal changes that yielded a well-known corkscrew appearance. This corkscrew appearance may have also obscured the detection of fine branches. In contrast, CHTA images could clearly depict intrahepatic arteries in any setting. Furthermore, we thought that the

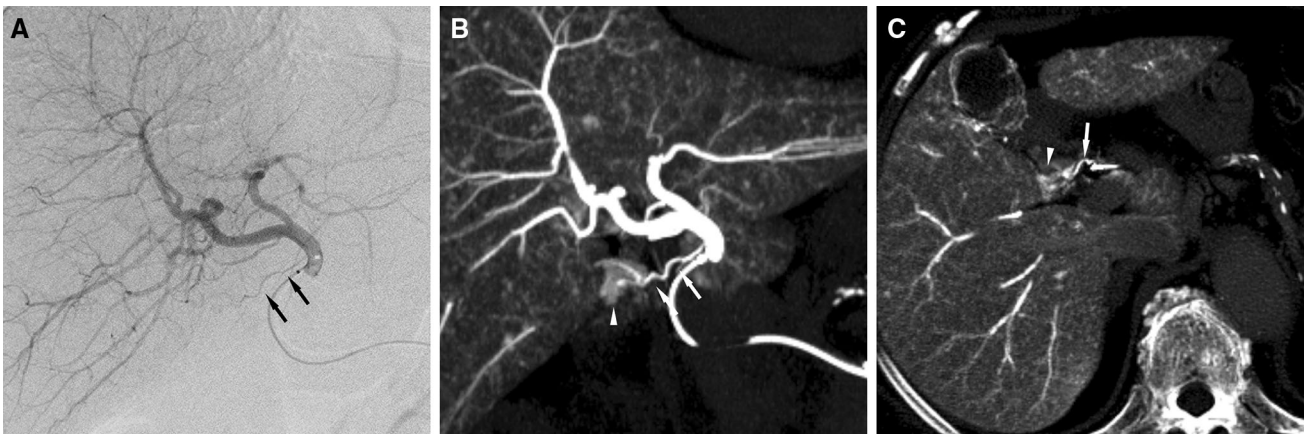

Fig. 5 Images of the duodenal artery in a 77-year-old woman with hepatitis C virus-related chronic hepatitis. **A** A branch arising from the proper hepatic artery (*black arrows*) was identified on the hepatic arteriogram, although the vascular territory was uncertain. Duodenal wall staining was unclear. **B** Coronal CT hepatic angiography (CTHA) image (maximum intensity projection) clearly shows the duodenal artery with its origin from the proper hepatic artery (*arrows*) and duodenal wall staining (*arrowhead*). **C** Axial CTHA image (maximum intensity projection) clearly shows the duodenal artery with its origin from the proper hepatic artery (*arrow*) and duodenal wall staining (*arrowhead*)

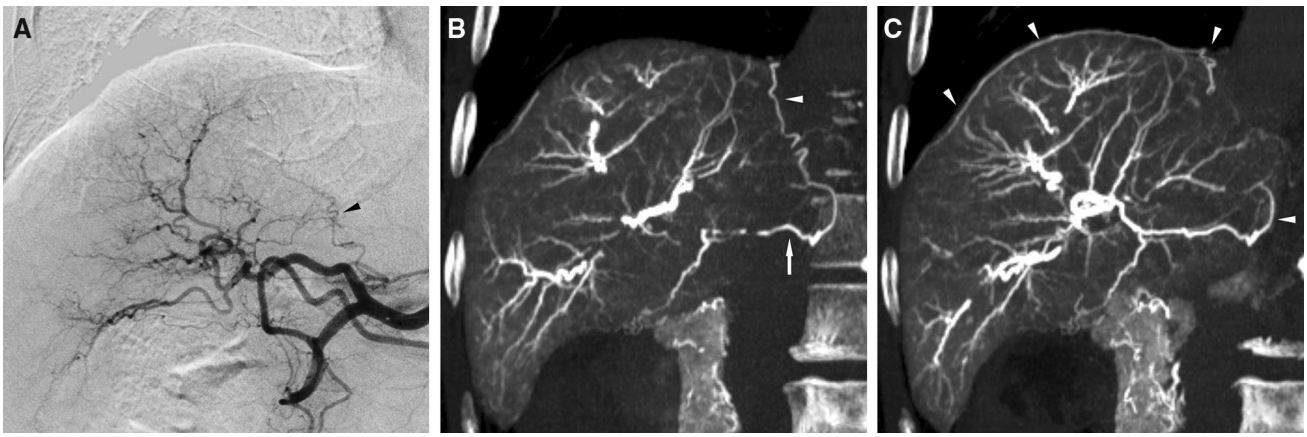

Fig. 6 Images of the right inferior phrenic artery in a 72-year-old woman with hepatitis C virus-related cirrhosis. **A** A branch arising from a hepatic branch (*black arrowhead*) was identified on the hepatic arteriogram, although the vascular territory was uncertain. **B**, **C** Coronal CT hepatic angiography (CTHA) images (maximum intensity projection) clearly show the branch arising from the caudate branch (A1, *arrow*) supplies the diaphragm (*arrowheads*)

non-diluted contrast medium was important to depict thin arteries. Therefore, we adapted the highly concentrated contrast material.

CHTA, which has no complementary modalities, is useful for detecting intrahepatic vasculature. In contrast, multidetector CT angiography and MR angiography cannot detect small branches [26], especially in cirrhotic livers, although detection using these modalities was previously reported in non-cirrhotic patients [27]. The catheter or contrast material used in cone-beam CT, a recent alternative method of obtaining cross-sectional images, may introduce artifacts in vessels that could impair the detection of fine intrahepatic structures; therefore, the temporal and spatial resolution of this modality may not be sufficient to detect small arteries [28]. Unfortunately, CHTA requires specialized instrumentation and radiation exposure and is thus relatively difficult to implement. Despite the challenges associated with routine CHTA examination at some institutions, the extrahepatic artery variability revealed in this study should contribute to the development of safer transarterial therapies and improved clinical outcomes.

Our study had some limitations. First, this was a retrospective study. Second, image evaluation was reviewed by a single radiologist. Third, we mainly interpreted CHA arteriograms, although peripheral branch detection rates may be increased through selective catheterization. However, we observed a definite and predominant ability of CTHA to detect branches mainly originating from proximal sites, such as the gastric, pancreatic, or duodenal branches. Fourth, we observed both the arteriogram and CTHA

Table 2 Sensitivity, specificity, and accuracy of arteriography for extrahepatic artery detection

	RGA	Falciform artery	Accessory LGA	Left IPA	PSPDA	Dorsal pancreatic artery	Duodenal artery	Right IPA
Sensitivity	80.0 (712/890)	53.9 (206/382)	64.6 (104/161)	76.7 (33/43)	100 (33/33)	57.7 (15/26)	8.3 (1/12)	0 (0/4)
Specificity	86.8 (46/53)	97.7 (548/561)	98.6 (771/782)	99.8 (898/900)	99.7 (908/911)	100 (917/917)	99.9 (930/931	100 (939/939)
Accuracy	80.4 (758/943)	80.0 (754/943)	92.3 (875/943)	98.7 (931/943)	99.9 (941/943)	98.8 (932/943)	98.7 (931/943)	99.6 (939/943)

RGA right gastric artery, *LGA* left gastric artery, *IPA* inferior phrenic artery, *PSPDA* posterior superior pancreaticoduodenal artery

images at slight different injection rates and contrast material volumes, which depended on the use of catheters. However, these differences may have an insignificant effect on image interpretation. Fifth, we could not statistically analyze the factors that caused poorer visualization of extrahepatic arteries on DSHA. Sixth, we used a relatively old data set because of the shift of the contrast material.

Conclusion

In conclusion, various extrahepatic arteries originating from hepatic arteries could be identified frequently on CTHA images. Notably, these arteries were frequently overlooked on DSHA. Clinicians should consider this potential of DSHA for poor visualization when investigating various types of arteries.

Acknowledgements We deeply appreciate the support of late Prof. Masayuki Suzuki (Department of Quantum Medical Technology, Graduate School of Medical Science, Kanazawa University, Kanazawa, Japan) toward our study.

Compliance with Ethical Standards

Conflict of interest All authors have no conflicts of interest and financial disclosures.

References

1. Matsui O, Kadoya M, Yoshikawa J, et al. Small hepatocellular carcinoma: treatment with subsegmental transcatheter arterial embolization. Radiology. 1993;188:79–83.
2. Yamakado K, Nakatsuka A, Takaki H, et al. Early-stage hepatocellular carcinoma: radiofrequency ablation combined with chemoembolization versus hepatectomy. Radiology. 2008;247:260–6.
3. Salem R, Lewandowski RJ, Atassi B, et al. Treatment of unresectable hepatocellular carcinoma with use of 90Y microspheres (TheraSphere): safety, tumor response, and survival. J Vasc Interv Radiol. 2005;16:1627–39.
4. Kim HC, Chung JW, Lee W, Jae HJ, Park JH. Recognizing extrahepatic collateral vessels that supply hepatocellular carcinoma to avoid complications of transcatheter arterial chemoembolization. Radiographics. 2005;25:S25–39.
5. Hirakawa M, Iida M, Aoyagi K, Matsui T, Akagi K, Fujishima M. Gastroduodenal lesions after transcatheter arterial chemoembolization in patients with hepatocellular carcinoma. Am J Gastroenterol. 1988;83:837–40.
6. Gibo M, Hasuo K, Inoue A, et al. Hepatic falciform artery: angiographic observations and significance. Abdom Imaging. 2001;26:515–9.
7. López-Benítez R, Radeleff BA, Barragán-Campos HM, et al. Acute pancreatitis after embolization of liver tumors: frequency and associated risk factors. Pancreatology. 2007;7:53–62.
8. Chung JW, Park JH, Han JK, Choi BI, Kim TK, Han MC. Transcatheter oily chemoembolization of the inferior phrenic artery in hepatocellular carcinoma: the safety and potential therapeutic role. J Vasc Interv Radiol. 1998;9:495–500.

9. Ishigami K, Yoshimitsu K, Irie H, et al. Accessory left gastric artery from left hepatic artery shown on MDCT and conventional angiography: correlation with CT hepatic arteriography. AJR Am J Roentgenol. 2006;187:1002–9.
10. Tajima T, Yoshimitsu K, Irie H, et al. Hepatic falciform ligament artery in patients with chronic liver diseases: detection on computed tomography hepatic arteriography. Acta Radiol. 2009;50: 743–51.
11. Burgmans MC, Too CW, Kao YH, et al. Computed tomography hepatic arteriography has a hepatic falciform artery detection rate that is much higher than that of digital subtraction angiography and 99mTc-MAA SPECT/CT: implications for planning 90Y radioembolization? Eur J Radiol. 2012;81:3979–84.
12. Matsui O, Kadoya M, Kameyama T, et al. Benign and malignant nodules in cirrhotic livers: distinction based on blood supply. Radiology. 1991;178:493–7.
13. Ueda K, Matsui O, Kawamori Y, et al. Hypervascular hepatocellular carcinoma: evaluation of hemodynamics with dynamic CT during hepatic arteriography. Radiology. 1998;206:161–6.
14. Hayashi M, Matsui O, Ueda K, et al. Correlation between the blood supply and grade of malignancy of hepatocellular nodules associated with liver cirrhosis: evaluation by CT during intraarterial injection of contrast medium. AJR Am J Roentgenol. 1999;172:969–76.
15. Williams DM, Cho KY, Ensminger WD, et al. Hepatic falciform artery: anatomy, angiographic appearance, and clinical significance. Radiology. 1985;156:339–40.
16. Song SY, Chung JW, Lim HG, Park JH. Nonhepatic arteries originating from the hepatic arteries: angiographic analysis in 250 patients. J Vasc Interv Radiol. 2006;17:461–9.
17. Lee AJ, Gomes AS, Liu DM, Kee ST, Loh CT, McWilliams JP. The road less traveled: importance of the lesser branches of the celiac axis in liver embolotherapy. Radiographics. 2012;32:1121–32.
18. Liu DM, Salem R, Bui JT, et al. Angiographic considerations in patients undergoing liver-directed therapy. J Vasc Interv Radiol. 2005;16:911–35.
19. Gwon DI, Ko GY, Yoon HK, et al. Inferior phrenic artery: anatomy, variations, pathologic conditions, and interventional management. Radiographics. 2007;27:687–705.
20. Nakamura H, Uchida H, Kuroda C, et al. Accessory left gastric artery arising from left hepatic artery: angiographic study. AJR Am J Roentgenol. 1980;134:529–32.
21. VanDamme JP, Bonte J. Vascular anatomy in abdominal surgery. Stuttgart: Georg Thieme Verlag; 1990. p. 33–42.
22. Ibukuro K, Tsukiyama T, Mori K, Inoue Y. Hepatic falciform ligament artery: angiographic anatomy and clinical importance. Surg Radiol Anat. 1998;20:367–71.
23. Bertelli E, Di GF, Bertelli L, Civeli L, Mosca S. The arterial blood supply of the pancreas: a review. II. The posterior superior pancreaticoduodenal artery. An anatomical and radiological study. Surg Radiol Anat. 1996;18:1–9.
24. Bertelli E, Di GF, Mosca S, Bastianini A. The arterial blood supply of the pancreas: a review. V. The dorsal pancreatic artery: an anatomic review and a radiologic study. Surg Radiol Anat. 1998;20:445–52.
25. Bianchi HF, Albanèse EF. The supraduodenal artery. Surg Radiol Anat. 1989;11:37–40.
26. Sahani D, Mehta A, Blake M, Prasad S, Harris G, Saini S. Preoperative hepatic vascular evaluation with CT and MR angiography: implications for surgery. Radiographics. 2004;24: 1367–80.
27. Ishigaki S, Itoh S, Satake H, Ota T, Ishigaki T. CT depiction of small arteries in the pancreatic head: assessment using coronal reformatted images with 16-channel multislice CT. Abdom Imaging. 2007;32:215–23.
28. Miyayama S, Matsui O, Yamashiro M, et al. Detection of hepatocellular carcinoma by CT during arterial portography using a cone-beam CT technology: comparison with conventional CTAP. Abdom Imaging. 2009;34:502–6.